Nuclear Instruments and Methods in Physics Research A 595 (2008) 88–91

Contents lists available at ScienceDirect

Nuclear Instruments and Methods in Physics Research A

journal homepage: www.elsevier.com/locate/nima

The DIRC detectors of the PANDA experiment at FAIR

K. Föhl [a,*], D. Bettoni [b], D. Branford [a], A. Britting [c], V. Carassiti [b], A. Cecchi [b], V.Kh. Dodokhof [d], M. Düren [e], M. Ehrenfried [e], W. Eyrich [c], D.I. Glazier [a], M. Hoek [f], R. Hohler [g], R. Kaiser [f], A. Lehmann [c], D. Lehmann [g], S. Lu [e], J. Marton [h], O. Merle [e], K. Peters [g], C. Pizzolotto [c], G. Rosner [f], G. Schepers [g], R. Schmidt [e], L. Schmitt [g], P. Schönmeier [e], C. Schwarz [g], B. Seitz [f], C. Sfienti [g], K. Suzuki [h], A. Teufel [c], A.S. Vodopianov [d], D.P. Watts [a]

[a] School of Physics and Astronomy, University of Edinburgh, Mayfield Road, Edinburgh EH9 3JZ, Scotland, UK
[b] INFN Ferrara, Via Paradiso 12, I-44100 Ferrara, Italy
[c] Physikalisches Institut IV, University of Erlangen-Nuremberg, Erwin-Rommel-Strasse 1, D-91058 Erlangen, Germany
[d] Laboratory of High Energies, Joint Institute for Nuclear Research, 141980 Dubna, Russia
[e] II. Physikalisches Institut, University of Giessen, Heinrich-Buff-Ring 16, D-35392 Giessen, Germany
[f] Department of Physics & Astronomy, Kelvin Building, University of Glasgow, Glasgow G12 8QQ, Scotland, UK
[g] Gesellschaft für Schwerionenforschung mbH, Planckstraße 1, D-64291 Darmstadt, Germany
[h] Stefan Meyer Institut für subatomare Physik, Austrian Academy of Sciences, A-1090 Vienna, Austria

ARTICLE INFO

Available online 22 July 2008

Keywords:
Particle identification
Cherenkov counter
Ring imaging

ABSTRACT

The PANDA experiment at the future Facility for Anti-proton and Ion Research (FAIR) aims at studying the strong interaction with antiprotons in the 1–15 GeV/c range. For the charged particle identification, in particular of kaons, one foresees two DIRC detectors. These will be located in the target spectrometer section of PANDA. A barrel shape DIRC with bar radiators will cover the central region, and a disc DIRC will be located in the forward endcap part. For the latter, two readout concepts are investigated: measuring the photon time-of-propagation in a multi-wavelength band disc DIRC, or measuring angles in a focussing lightguide dispersion-correcting disc DIRC.

The PANDA[1] experiment [1] at the future FAIR laboratory is a fixed target experiment scattering cooled antiprotons circulating in the High Energy Storage Ring (HESR) with momenta of 1–15 GeV/c off an internal pellet or gas jet target at interaction rates of up to 2×10^7/s to perform high precision experiments in the charmed quark sector. The target spectrometer section, with a superconducting solenoid and most subdetectors housed inside the return yoke, covers the acceptance except for a hole of $\vartheta = 10^\circ$ (horizontal) and $\vartheta = 5^\circ$ (vertical) in the forward direction. This opens towards a dipole providing additional bending power and the subdetectors of the forward spectrometer section.

Two DIRCs[2] are foreseen as dedicated detectors for the charged particle identification (PID) of the PANDA experiment. For the PID, their information will be combined with adjacent tracking and calorimetry detectors.

1. DIRC detectors

The PANDA target spectrometer (see Fig. 1) is almost hermetically sealed to avoid solid angle gaps, and to keep material volume low, there is little spare space inside. The possibility of using thin radiators and placing the readout elements outside the acceptance, and potentially outside the magnet return yoke, favours the use of DIRC designs as Cherenkov imaging detectors for PID.

With the momentum ranges anticipated for the physics reactions in PANDA (Fig. 2 shows one of the benchmark reactions), the demands on the separation power increase towards forward angles. The detectors cover different angular ranges, and hence the required performance is different.

Each of the DIRC designs suggested for PANDA has to improve over currently implemented DIRC designs, and hence needs to address the effects of chromatic dispersion of the Cherenkov light emission. For the time-of-propagation Endcap DIRC design, selecting a narrow wavelength band limits the group velocity time spread. For the optical imaging Endcap DIRC design, a prism element can largely correct the dispersion angle spread.

The detectors are being located in a high radiation area. Regarding the radiator material, proton beam irradiation up to

* Corresponding author.
E-mail address: kf@ph.ed.ac.uk (K. Föhl).
[1] antiProton ANnihilation at DArmstadt.
[2] Detector of Internally Reflected Cherenkov light.

0168-9002/$ - see front matter © 2008 Elsevier B.V. All rights reserved.
doi:10.1016/j.nima.2008.07.094

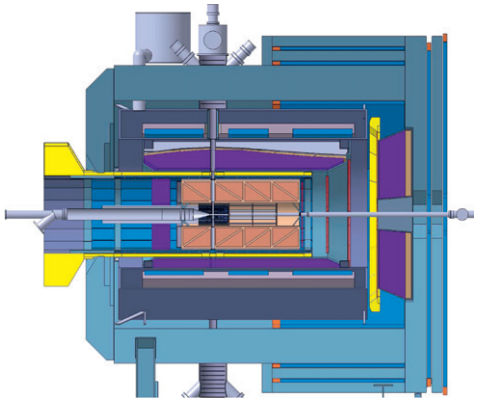

Fig. 1. PANDA target spectrometer. The Barrel and the Endcap DIRC detector positions are shown in light colour.

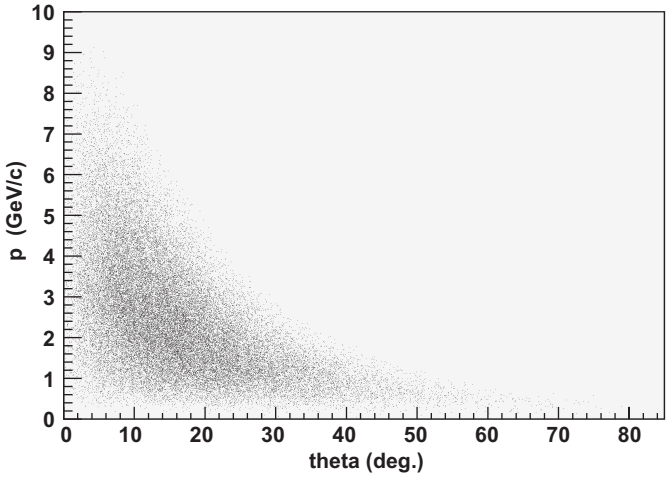

Fig. 2. Acceptance plot for kaons from the $p\bar{p} \to \psi_h \eta$ reaction at $p\bar{p} = 15\,\mathrm{GeV}/c$. The Barrel DIRC covers $\vartheta = 22^\circ - 140^\circ$, the Endcap DIRC the more forward range $\vartheta = 5^\circ - 22^\circ$.

10 Mrad [2] shows that amorphous fused silica is radiation-hard. Several photon detector types are being tested, to find whether they stand a high magnetic field of $B \approx 2\,\mathrm{T}$ [3] and high photon rates.

2. Barrel DIRC

The DIRC in the barrel part covers the angular range from $\vartheta = 22^\circ$ to 140°. The design is initially based on a scaled version of the BaBar DIRC [4]. In order to improve performance, combining the time of arrival of the photons with their spatial image determines not only the particles velocity, but also the wavelength of the photons. Therefore, dispersion correction at the lower and upper detection thresholds is possible. See the separate paper [5] in these proceedings for details of the PANDA Barrel DIRC.

In addition the development of a smaller photon detector is going on, which is easier to integrate within the complete detector set-up: a photon detector coupled with a small air gap to the radiator slabs with focussing lenses. This reduces image distortions, sorts out large angle photons deteriorating the Cherenkov image, and also allows for a more simple integration of the photon detector in the complete set-up: due to the air gap the photon detector can be easily removed and reconnected. Efforts are taken to produce a small-scale prototype.

3. Endcap DIRC

Two DIRC design options exist for the endcap part of the target spectrometer section. These differ in the photon readout design but both use an amorphous fused silica radiator disc. The endcap detector position covers forward angles of up to $\vartheta = 22^\circ$ excluding an inner rectangular area of $\vartheta_x = 10^\circ$ horizontal and $\vartheta_y = 5^\circ$ vertical half-angles. Simulations using the DPM generator [6] give 1.0 ± 0.8 (at $2\,\mathrm{GeV}/c$) to 2.3 ± 1.8 (at $15\,\mathrm{GeV}/c$) charged particle multiplicity per $\bar{p}p$ interaction emitted from the target vertex into this acceptance.

In such a one-dimensional[3] DIRC type, a photon is transported to the edge of a circular disc while preserving the angle information. Avoiding too much light scattering loss at the surface reflections requires locally (in the order of millimetres) a surface roughness not exceeding several nanometres RMS.

The lower velocity threshold, which is common to both designs, depends on the onset of total internal reflection for a part of the photons emitted in the Cherenkov cone.

3.1. Time-of-Propagation disc DIRC

In the Multi-Chromatic Time-of-Propagation design (see separate paper [7] for details) small detectors measure the arrival time of photons on the disc rim, requiring $\sigma_t = 30-50\,\mathrm{ps}$ single photon time resolution.

For any given wavelength, the disc edge is effectively covered alternately with mirrors and detectors. Only due to the resulting different light path-lengths one can determine accurately enough the start reference time, i.e. the time when the initial charged particle enters the radiator, as the stored antiproton beam in the HESR has no suitable time structure to be used as an external time start.

As some of the light is reflected several times before hitting a detector, the longer path lengths allow a better relative time resolution.

The use of dicroic mirrors as colour filters allows the use of multiple wavelength bands within the same radiator (the current design suggesting two bands) resulting in higher photon statistics. The narrow wavelength bands minimise the dispersion effects, and the quantum efficiency curve of the photocathode material could be optimised for each wavelength band individually.

3.2. Focussing lightguide disc DIRC

In the Focussing Lightguide Dispersion-Correcting design (Figs. 3 and 4), when a photon arrives at the edge of the circular or polygonal disc, it enters into one of about 100 optical elements on the rim. Here, the two-fold angular ambiguity (up-down) is lifted, the chromatic dispersion corrected and the photon focussed onto a readout plane. While the optical element entered determines the ϕ coordinate, measuring the position in the dispersive direction on the focal plane of the focussing lightguide yields the θ coordinate.

Lithium fluoride (LiF) is UV transparent and has particularly low dispersion. Proton beam irradiation of a test sample shows that radiation-produced colour centres are confined to sufficiently small wavelength ranges, and are only partially absorbing at the expected PANDA lifetime dose. Hence, we believe we can use LiF as a prism element (see Fig. 4) to correct the Cherenkov radiation dispersion. The two boundary surfaces, with the radiator disc and

[3] Light is only reflected on surfaces of one spatial orientation, here the two disc surfaces both normal to the z-axis.

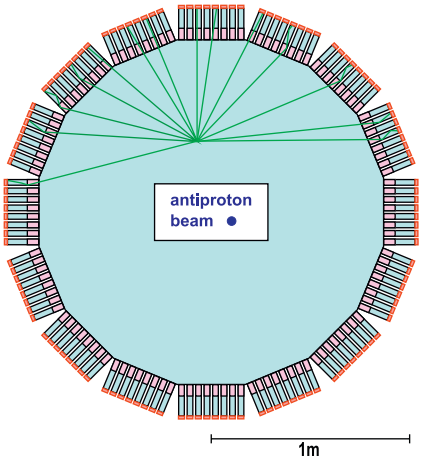

Fig. 3. Polygonal disc with focussing lightguides attached to the rim used as optical readout components.

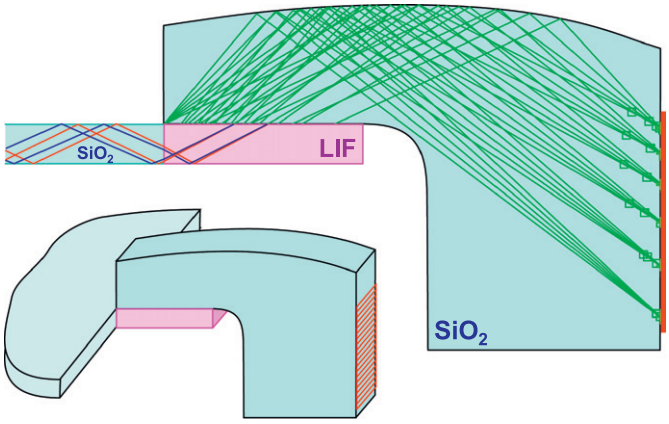

Fig. 4. Lightguide side view (inset three-dimensional visualisation) shown with a set of rays used for optimising the lightguide curvature. Reflections at the parallel front and back surfaces keep the light inside but do not affect the focussing properties.

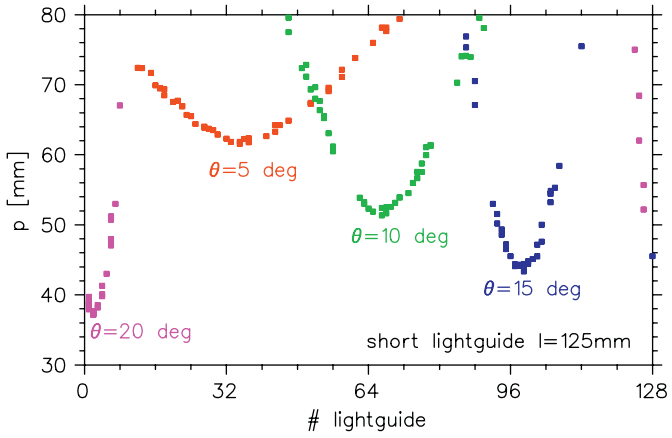

Fig. 5. Simulated photon hit pattern for four particles emitted at different angles θ and ϕ from the target vertex.

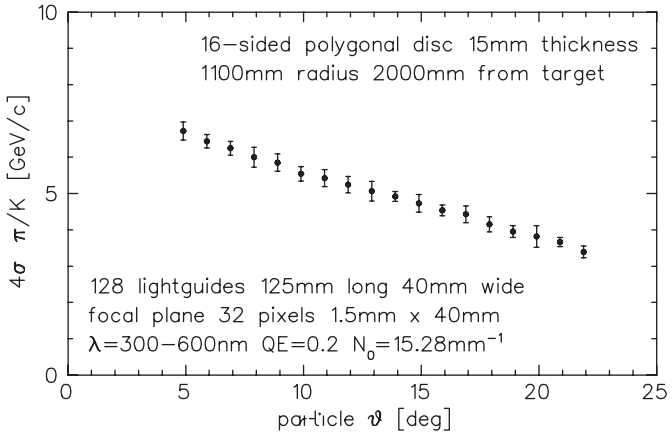

Fig. 6. Simulation-derived pion–kaon separation power for a focussing lightguide design with a 15 mm thick amorphous fused silica disc and 0.4 eV photodetector efficiency.

the subsequent lightguide, make the chromatic dispersion correction angle-independent to first order.

As with the radiator, the light impinging on the inside of the lightguide's curved surface undergoes total internal reflection, hence no mirror coating is needed (see Fig. 4). This reflection makes the focussing also independent of the wavelength.

With the light staying within the dense optical material of the lightguide, most of the incoming light phase space from the disc is mapped onto the focal plane with its one-coordinate readout. The focussing surface with cylindrical shape of varying curvature has been optimised to give an overall minimum for the focus spot sizes of the different angles on the focal plane, individual standard deviations being well below 1 mm for the instrumented area.

3.3. Optical simulations

Charged particles emitting Cherenkov radiation and photon propagation have been simulated as shown here for the focussing lightguide design, and the detector resolution derived in analysing the photon hit patterns (see Fig. 5).

The charged particle trajectory includes angular straggling, and the wavelength dependence of the refractive indices is parametrised with Sellmeier coefficients. Examples of idealisations: perfectly parallel disc surfaces, no bulk light absorption and 100% reflectivity for total internal reflection (can be investigated separately), no detector noise or light from background particles.

Typically all of the 40 detected photons per particle (each with $\sigma_t = 0.1$ ns) arrive within a 4 ns time window. For the pixel size used in this simulation they are contained inside a 40 pixel ns volume.

The photon pattern analysis is seeded with particle vertex information, smeared to the resolution of the upstream tracking detectors. Differential response vectors are computed, one tracking parameter offset at a time, with high photon statistics using the simulation code. Particle vertex parameters and velocity are then fitted simultaneously.

Event sets are recorded for two different particle types A and B of same momentum. The detector resolving power is then derived from the mean m and standard deviation σ of $\beta = v/c$, with the sigma separation value defined as

$$\sigma_{\mathrm{SEP}} = \frac{|m_A - m_B|}{\sigma_\beta} = \frac{|m_A - m_B|}{(\sigma_A/2 + \sigma_B/2)}.$$

For an Endcap DIRC detector with 128 lightguides and 4096 detector pixels that fits inside the target spectrometer return

yoke, Fig. 6 shows the angle-dependent upper momentum limit being 4–6 GeV/c for 4σ pion–kaon separation within the acceptance $\vartheta = 5^\circ - 22^\circ$.

4. Conclusions

The compactness of the PANDA detector requires novel detectors for the particle identification. We propose several DIRC detector designs for pion–kaon separation that fit into the limited space of the target spectrometer. The overall performance of the detector components has to exceed that of existing DIRC models to stand the very high antiproton rates and a harsh radiation environment.

Acknowledgements

This work is supported by EU FP6 grant, contract number 515873, DIRACsecondary-Beams.

References

[1] PANDA Collaboration, Technical Progress Report, FAIR–ESAC/Pbar, 2005.
[2] M. Hoek, et al., Nucl. Instr. and Meth. A 595 (2008) 190.
[3] A. Lehmann, et al., Nucl. Instr. and Meth. A 595 (2008) 173.
[4] R. Alexsan, et al., Nucl. Instr. and Meth. A 397 (1997) 261.
[5] C. Schwarz, et al., Nucl. Instr. and Meth. A 595 (2008) 112.
[6] A. Galoyan, V.V. Uzhinsky, AIP Conference Proceedings 796, 2005, pp. 79–82.
[7] P. Schönmeier, et al., Nucl. Instr. and Meth. A 595 (2008) 108.